

1 **Evaluation of machine learning techniques with multiple remote sensing datasets in**
2 **estimating monthly concentrations of ground-level PM_{2.5}**

3

4 Authors: Yongming Xu¹, Hung Chak Ho², Man Sing Wong^{2,3}, Chengbin Deng⁴, Yuan Shi⁵, Ta-
5 Chien Chan⁶, Anders Knudby⁷

6 1. School of Remote Sensing and Geomatics Engineering, Nanjing University of Information
7 Science & Technology, Nanjing, China

8 2. Department of Land Surveying and Geo-Informatics, The Hong Kong Polytechnic
9 University, Kowloon, Hong Kong

10 3. Research Institute for Sustainable Urban Development, The Hong Kong Polytechnic
11 University, Hong Kong

12 4. Department of Geography, State University of New York at Binghamton, Binghamton,
13 New York, United States

14 5. School of Architecture, Chinese University of Hong Kong, New Territories, Hong Kong

15 6. Research Center for Humanities and Social Sciences, Academia Sinica, Taiwan

16 7. Department of Geography, Environment and Geomatics, University of Ottawa, Ottawa,
17 ON, Canada

18

19 Corresponding Author: Hung Chak Ho, Department of Land Surveying and Geo-Informatics,
20 Hong Kong Polytechnic University, Hong Kong

21

22

23 **Abstract**

24 Fine particulate matter (PM_{2.5}) has been recognized as a key air pollutant that can
25 influence population health risk, especially during extreme cases such as wildfires. Previous
26 studies have applied geospatial techniques such as land use regression to map the ground-
27 level PM_{2.5}, while some recent studies have found that Aerosol Optical Depth (AOD) derived
28 from satellite images and machine learning techniques may be two elements that can improve
29 spatiotemporal prediction. However, there has been a lack of studies evaluating use of
30 different machine learning techniques with AOD datasets for mapping PM_{2.5}, especially in
31 areas with high spatiotemporal variability of PM_{2.5}.

32 In this study, we compared the performance of eight predictive algorithms with the use of
33 multiple remote sensing datasets, including satellite-derived AOD data, for the prediction of
34 ground-level PM_{2.5} concentration. Based on the results, Cubist, random forest and eXtreme
35 Gradient Boosting were the algorithms with better performance, while Cubist was the best
36 (CV-RMSE=2.64 µg/m³, CV-R²=0.48). Variable importance analysis indicated that the predictors
37 with the highest contributions in modelling were monthly AOD and elevation.

38 In conclusion, appropriate selection of machine learning algorithms can improve ground-
39 level PM_{2.5} estimation, especially for areas with nonlinear relationships between PM_{2.5} and
40 predictors caused by complex terrain. Satellite-derived data such as AOD and land surface
41 temperature (LST) can also be substitutes for traditional datasets retrieved from weather
42 stations, especially for areas with sparse and uneven distribution of stations.

43

44 **1. Introduction**

45 Fine particulate matter (PM_{2.5}) is one of the major dust-related air pollutants that can
46 increase morbidity and mortality risks, especially for cardiovascular and respiratory issues
47 (Atkinson et al., 2014). In order to reduce community health risks caused by environmental
48 exposure, previous studies have commonly applied air quality data from single or a small
49 number of monitoring stations to evaluate the temporal influences of PM_{2.5} (Liu et al., 2018;
50 Ostro et al., 2014; Wang et al., 2017), and have found positive association between PM_{2.5} and
51 chronic diseases. These results have helped pinpoint air pollution as a severe community
52 health problem (Kan et al., 2012). However, sparse distribution of air quality monitoring
53 stations across large areas reduces the ability to demonstrate the actual impact of PM_{2.5} on all
54 vulnerable populations.

55 Satellite remote sensing data can provide spatially continuous estimates of aerosol optical
56 depth (AOD), providing an alternative method to map ground-level PM_{2.5} across a large region.
57 Since AOD from satellite images has complete spatial coverage and moderate spatial
58 resolution, AOD measurement can fill in data for areas that lack monitoring stations. Multiple
59 studies have been carried out to estimate PM_{2.5} from satellite-derived AOD and other
60 environmental variables (Lai et al., 2014; Saunders et al., 2014; Wu et al., 2015). Due to the
61 spatio-temporal heterogeneity of AOD-PM_{2.5} relationships, using AOD to directly represent
62 ground-level PM_{2.5} may be inappropriate, as has been reported by previous studies (Lee et al.,
63 2011; Paciorek et al., 2008). Additional environmental predictors, such as geographical and
64 meteorological variables, have also been incorporated in models to improve estimation
65 performance (Hu et al., 2013; Kloog et al., 2011; Liu et al., 2009). To derive PM_{2.5} from satellite-

66 derived AOD and other predictors, various models have been developed. The most commonly
67 used models include multiple linear regression (Lai et al., 2014; Liu et al., 2004; Saunders et
68 al., 2014; Schaap et al., 2009; Yao et al., 2018a), mixed effect models (Just et al., 2015; Lee et
69 al., 2011; Zheng et al. 2016; Xie et al., 2015), chemical transport models (Crouse et al., 2016;
70 Wang & Chen, 2016; van Donkelaar et al., 2006) and geographically weighted regression (Chu
71 et al., 2015; Chu et al., 2016; He and Huang, 2018; Jiang et al., 2017; Ma et al., 2014; Shi et al.,
72 2018; Song et al., 2014; Wu et al., 2016; You et al., 2016). Recently, machine learning
73 technology, which can fit complicated non-linear relationships in many dimensions, has also
74 been employed to derive air-pollutant concentrations from remote sensing data (Chen et al.,
75 2018; Deters et al., 2017, He & Huang, 2018, Yao et al., 2018b). Several machine learning
76 methods, such as artificial neural networks, generalized boosting models, support vector
77 machine and random forest, have also been used to generate models for estimating PM_{2.5} (Di
78 et al., 2016; Hu et al., 2017; Reid et al., 2015; Zhan et al., 2017). However, to date, studies with
79 machine learning for estimating PM_{2.5} are still rare in this field.

80 In order to better understand the potential of machine learning for PM_{2.5} mapping, we
81 developed an innovative approach to estimate spatial variability of PM_{2.5} by using machine
82 learning techniques with multiple predictors based on Moderate Resolution Imaging
83 Spectroradiometer (MODIS) and re-analysis data. By using machine learning techniques, it can
84 better include non-linear relationships for estimating air pollution based on all geophysical
85 components. To enhance the ability to develop a spatiotemporal model for PM_{2.5} prediction,
86 the specific objectives of this study included 1) to develop a model for predicting PM_{2.5} based
87 on remote sensing data, re-analysis data and station observed air quality data; 2) to evaluate

88 the prediction performance of different statistical methods, for determining the best model
89 setting for estimating $PM_{2.5}$; and 3) to map the spatio-temporal distribution of $PM_{2.5}$ based on
90 the best model. British Columbia of Canada was selected as the case of this study, because of
91 its complex terrain and wildfire history that can significantly influence air quality across the
92 province, including $PM_{2.5}$.

93 **2. Study Area**

94 British Columbia (BC) is the westernmost province of Canada (Fig. 1), and it is characterized
95 by mountainous terrain and heavy forest cover. BC has traditionally been known for its clean
96 environment. However, due to climate change, increasing frequency of wildfires has been
97 observed in recent decades (Wildfire Management Branch, 2014; Wotton, 2010). Wildfires
98 produce excessive smoke that can influence regional air quality and severely affect human
99 health (Henderson et al., 2011; McLean et al., 2015; Krstic & Henderson et al., 2015). In order
100 to minimize air pollution risk, a National Air Pollution Surveillance (NAPS) system with ground-
101 based stations has been established across the province, monitoring temporal changes in air
102 pollutants including the daily change in $PM_{2.5}$. However, due to the province's sprawling
103 territory with complex terrain and a limited number of surveillance stations, station-based
104 observation may not be able to adequately measure the $PM_{2.5}$ influencing all populated
105 regions (McLean et al. 2015). The stations with data between 2001 and 2014 were sparsely
106 distributed and clustered in the southern and central parts of BC. Therefore, combining
107 satellite images to monitor the spatiotemporal changes in $PM_{2.5}$ across the province is essential.

108 3. Data and Methods

109 3.1 Selection of predictors for PM_{2.5} mapping

110 According to previous studies, AOD has strong positive relationships with ground-level
111 PM_{2.5} concentrations (Engel-Cox et al., 2004; Mukai et al., 2006; Wang & Christopher, 2003;
112 Xin et al., 2014), and some studies have applied satellite-derived AOD to map PM_{2.5} (Chu et al.,
113 2016). Therefore, AOD was the first predictor for PM_{2.5} mapping. In this study, AOD data were
114 retrieved from MOD04_3K, a 3-km near-real-time aerosol dataset derived from TEAAR/MODIS.

115 Based on previous studies, the PM_{2.5}-AOD relationship can be a multivariate function of
116 a wide range of influencing factors (Lary et al., 2015; Natunen et al., 2010; Song et al., 2014;
117 van Donkelaar et al., 2006). For example, meteorological and geographical predictors can be
118 the parameters of co-predicting PM_{2.5} concentrations (Jiang et al., 2017; Liu et al., 2009; Ma
119 et al., 2014; Reid et al., 2015; You et al., 2016). Based on a search of the literature, the following
120 parameters may contribute to PM_{2.5} prediction: humidity, temperature, albedo, normalized
121 difference vegetation index (NDVI), height of the planetary boundary layer (HPBL), wind speed,
122 distance to the ocean, elevation, and calendar month. Therefore, we constructed the input
123 datasets for modelling as follows.

124 Considering the bias which sparse distribution of weather stations may produce in data
125 representing spatial variations in temperature and humidity, 26855 images of MODIS land
126 surface temperature product (MOD11A1) and 44336 images of MODIS water vapor product
127 (MOD05_L2) were used as alternatives to relative humidity and air temperature for better
128 spatial representativeness. In brief, MOD11A1 is a 1-km daily land surface temperature (LST)
129 product derived from TERRA/MODIS, and MOD05_L2 is a 1-km near-real-time water vapor

130 product derived from TERRA/MODIS.

131 In addition, NDVI and albedo were derived based on MODIS products: the MODIS
132 vegetation index product (MOD13A3), a 1-km monthly vegetation index product derived from
133 TERRA/MODIS; and the MODIS albedo product (MCD43B3), a 1-km 8-day albedo product
134 derived from TERRA/MODIS and AQUA/MODIS. For the mapping purpose, all MODIS datasets
135 were re-projected to the Albers projection, resampled to 1-km spatial resolution, and averaged
136 for each month.

137 Finally, HPBL and wind speed were derived from NCAR/NCEP re-analysis data, which
138 provides the corresponding data on a monthly basis. Elevation was derived from a digital
139 elevation model (DEM) dataset of the Shuttle Radar Topography Mission (SRTM). Distance to
140 the ocean was calculated by buffer analysis based on the coastal boundary of BC.

141 Based on the satellite-derived products and re-analysis data, a total of 10 predictors were
142 employed to estimate ground-level PM_{2.5} concentration across BC: monthly AOD, monthly
143 vapor, monthly LST, monthly HPBL, monthly wind speed, monthly NDVI, monthly albedo,
144 elevation, distance to ocean and calendar month (Table 1).

145 It is known that the relationship between environmental predictors and PM_{2.5} may vary
146 across space (Hu et al., 2013; Song et al., 2014), as well as time. We did not include spatial
147 predictors (e.g. latitude, longitude) other than “distance to ocean”, and we did not use
148 spatially weighted models such as geographically weighted regression, because of the limited
149 insight that can be gained from using such predictors/models, and the limited transferability
150 such models will have to other geographical regions.

151 **3.2 Model development with machine learning algorithms**

152 Association between $PM_{2.5}$ concentration of air quality monitoring stations and the
153 values of predictors retrieved by the locations of stations were first established for each
154 machine learning model in order to estimate the spatial distributions of ground-level $PM_{2.5}$
155 concentrations. In this study, ground-level $PM_{2.5}$ concentrations for modelling were retrieved
156 from 63 stations of the NAPS network operated by Environment Canada, with hourly $PM_{2.5}$
157 data between 2001 and 2014 across BC. Since several stations within this study period did not
158 provide temporal-continuous observations, or even had significant data gaps in temporal
159 observation, we averaged hourly $PM_{2.5}$ data on a daily basis, then converted the daily
160 information to the monthly average $PM_{2.5}$ concentrations based on all valid daily values.

161 These monthly average $PM_{2.5}$ values across BC province were then applied to the
162 following statistic algorithms to construct the regression models: 1) multiple linear regression
163 (MLR); 2) Bayesian Regularized Neural Networks (BRNN), 3) Support Vector Machines with
164 Radial Basis Function Kernel (SVM), 4) Least Absolute Shrinkage and Selection Operator
165 (LASSO), 5) Multivariate Adaptive Regression Splines (MARS), 6) Random forest (RF) (Breiman,
166 2001), 7) eXtreme Gradient Boosting (XGBoost), and 8) Cubist (RuleQuest, 2016).

167 MLR is a widely used algorithm in remote sensing applications because of its simplicity,
168 but it relies on several assumptions concerning data distributions, and its performance
169 depends on meeting these assumptions as well as the linearity of the modeled relationship
170 (Helsel and Hirsch 1992). BRNN is a back-propagation network that based on a mathematical
171 technique named Bayesian regularization to convert nonlinear regression into “well-posed”
172 problems (Burden and Winkler, 2008). It is more robust than standard back-propagation neural

173 networks. SVM was originally developed for classification by constructing separating
174 hyperplanes to define decision boundaries, and later expanded for regression. To map samples
175 to high dimension space, kernel functions were introduced. The radial basis function showed its
176 advances of handling nonlinear problems and fewer tunable parameters (Hsu, 2003; Bennett and
177 Campbell, 2000). LASSO is a regularization and variable selection method which shrinks coefficients
178 by forcing some less important coefficients to zero (Tibshirani, 1996). It can improve the model
179 interpretability and reduce overfitting. MARS is a fully automated method based on the divide-
180 and-conquer strategy, in which the training dataset is split into piecewise linear segments
181 (splines) (Friedman, 1991). RF is an ensemble-based decision tree approach, which consists of
182 a combination of decision trees fitted by randomly selected subsets of training samples. Final
183 predictions produced by RF model are determined by the average of the results of all the trees
184 (Breiman, 2001). XGBoost is an ensemble tree method which follows the principle of Gradient
185 boosting framework (Friedman, 2001), and uses regularization techniques to control
186 overfitting and model complexity (Chen and Guestrin, 2016). Cubist is a rule-based tree model,
187 which produces multiple linear regression models in the terminal nodes of trees based on the
188 M5 theory (Quinlan, 1992). A prediction at the terminal node is made by the corresponding
189 linear regression model and is smoothed by combining with predictions from nearest-neighbor
190 nodes within the tree to improve prediction accuracy (Houborg & McCabe, 2018). In addition,
191 Cubist also constructs multiple tree models (called committees), each of which consists of a
192 set of rule-based models (John et al., 2018). Predictions from all the committees are averaged
193 to produce the final prediction.

194 Except for the widely-used traditional MLR algorithm, others were machine learning

195 algorithms, which can effectively fit nonlinear and complex relationships between outcomes
196 and predictors (Ngufor et al. 2015). In this study, the complex terrain of the study area can
197 form a nonlinear relationship between ground-level PM_{2.5} concentrations and all predictors,
198 for which machine learning models may provide better results.

199 In order to optimize the PM_{2.5} estimation, parameter values were adjusted in each
200 machine learning model with a fitting process, based on the determination of the best
201 parameters by cyclic testing with committees of 1, 5, 10, 20, 50, and neighbors of 0, 1, 5, 9. In
202 addition, predictions of PM_{2.5} concentrations with all machine learning models were
203 conducted with the R (R Development Core Team).

204 **3.3 Model evaluation**

205 10-fold cross-validation was performed to evaluate the accuracy of all machine learning
206 models. Data were first randomly divided into 10 subsets, with one of the subsets used as the
207 validation dataset and the remaining used as training datasets; then repeating 10 times until
208 all subsets have been used as validation datasets once. Root-mean-square error (CV-RMSE)
209 and coefficient of determination (CV-R²) based on the comparison of validation and training
210 data were used to evaluate the accuracy of each machine learning model. While the best
211 model for PM_{2.5} estimation was determined based on the accuracies, variable importance
212 analysis was also conducted to evaluate the contributions of each predictor in PM_{2.5} estimation,
213 based on the determination of percentage increase in mean square error (%IncMSE) of each
214 model relative to the original error, after a predictor was randomly permuted. A higher value
215 of %IncMSE indicated higher importance of this corresponding predictor to the estimation.

216 **4. Results**

217 **4.1 Empirical relationship between PM_{2.5} and AOD**

218 A total of 1242 records of observed data of ground-level PM_{2.5} concentrations were
219 retrieved from stations with effective monthly AOD values based on location. In brief, PM_{2.5}
220 concentrations of this subset ranged from 1.26µg/m³ to 51.14µg/m³, with an average of
221 5.26µg/m³ and a median of 4.58µg/m³. This indicated a clean environment with low air
222 pollution during the study period across BC, except in a few extreme cases. Based on the
223 observed data, the extremes in PM_{2.5} concentration samples were observed in August 2003
224 and August 2010, when there were wildfire events (e.g. 2003 Okanagan Mountain Park Fire)
225 across BC.

226 A positive but poor correlation was observed based on evaluation of an empirical
227 relationship between observed PM_{2.5} and satellite-derived AOD (Fig. 2), with a correlation
228 coefficient (R) of 0.34 (P-value < 0.01), a clustering of data was found with AOD value less than
229 0.8 and PM_{2.5} value less than 15µg/m³. Observed data with moderate or high values were
230 scattered, possibly due to the complexity of the atmospheric conditions and landscapes across
231 BC. Similar evidence has also been found in a previous study, which demonstrated a non-linear
232 relationship between geophysical environment and air temperature across BC (Xu et al., 2014).
233 Therefore, the use of simple linear regression for ground-level PM_{2.5} estimation is insufficient
234 and inaccurate, and nonlinear multivariate models should be adopted to predict PM_{2.5} under
235 consideration of relevant atmosphere-surface interactions.

236 **4.2 Model performance**

237 Parameters of machine learning models were optimized with the fitting process, by cyclic

238 testing with a given parameter range and step size. Based on the results of optimized models,
239 CV-RMSE ranged from 2.64 $\mu\text{g}/\text{m}^3$ to 3.24 $\mu\text{g}/\text{m}^3$ and CV-R² ranged from 0.22-0.49 (Table 2).
240 Among all, RF, XGBoost and Cubist were the models with better performance, while Cubist had
241 the best performance determined by CV-RMSE. With 20 committees and 5 neighbors as
242 optimal parameters, CV-RMSE and CV-R² of Cubist were 2.64 $\mu\text{g}/\text{m}^3$ and 0.48. In contrast, MLR
243 method had the lowest performance (CV-RMSE=3.24 $\mu\text{g}/\text{m}^3$ and CV-R²=0.22), indicating its
244 poor capability of capturing complex relationships for the study area.

245 For the best model, the predicted and observed values were well aligned with the line of
246 best fit (Fig. 3), indicating the high accuracy of PM_{2.5} estimation with Cubist. However,
247 underestimation was also found for observed data with high PM_{2.5} values (> 20 $\mu\text{g}/\text{m}^3$), possibly
248 due to the small sample size, resulting in inability to robustly predict these high-value data
249 with a decision-based machine learning algorithm. Moreover, average deviation of PM_{2.5}
250 estimation was 0.07 $\mu\text{g}/\text{m}^3$, slightly higher than the deviation of observed values. These results
251 show that lower PM_{2.5} concentration in observed data may result in overestimation, while
252 higher values in observed data might result in underestimation during prediction.

253 **4.3 Variable importance analysis**

254 Based on the variable importance analysis, the predictors with highest contributions to
255 the Cubist model were monthly AOD and elevation. %IncRMSE without monthly AOD as
256 predictor was 12.14%, possibly due to its strong association between AOD and ground-level
257 air quality. %IncRMSE without elevation as a predictor was 9.26%, also suggesting a high
258 importance in PM_{2.5} estimation because of the influences of complex terrain in BC, with great
259 variations in altitude between the coast and interior. However, there shall be several factors

260 which contributed to the importance of elevation for predictions of PM_{2.5}: areas with high
261 elevation are inclined to suffer from wildfires; areas with low elevation tend to be influenced
262 by human activities. As AOD is an important predictor in the models, elevation may be used
263 to correct for model predictions. In addition, %IncRMSE of monthly albedo, monthly LST and
264 calendar month ranged from 4% to 6%. Predictors with the least importance were monthly
265 wind speed, monthly HPBL, monthly vapor and monthly NDVI, with a range of %IncRMSE
266 between 2% and 4%.

267 **4.4 Determination of location-based error**

268 To further determine the spatial variability of error, RMSEs were extracted by the location
269 of each station (Fig. 4). Most stations had RMSEs lower than 2.0µg/m³, while the stations with
270 the lowest RMSEs were in southeastern, western and southwestern BC. In contrast, high errors
271 were found at stations located in central and central-southern parts of BC, with RMSEs ranging
272 from 3.0 - 4.0µg/m³ or even higher. Compared with the DEM, these stations with higher RMSEs
273 were in mountainous valleys with high PM_{2.5} concentrations. Estimation errors of these
274 stations were mostly negative, indicating an underestimation of ground-level PM_{2.5} across
275 these valleys. These were also aligned with previous findings (Fig. 3) that observed data with
276 higher PM_{2.5} may introduce a higher chance of underestimation based on the Cubist model in
277 this study.

278 **5 Discussion**

279 **5.1 Spatiotemporal variability of ground-level PM_{2.5} concentration**

280 Based on the average concentrations of ground-level PM_{2.5} between 2001 and 2014 (Fig.
281 6), considerable spatial heterogeneity was found across BC. Generally, northern and

282 northeastern BC were areas with lower PM_{2.5} concentrations (< 4 µg/m³), while mountainous
283 regions across western BC were areas with higher concentrations of PM_{2.5} (5-6 µg/m³). We
284 also observed several extreme cases in mountainous valleys of BC (>7 µg/m³). One reason for
285 this spatiotemporal variability might be associated with wildfires, as this was a major source
286 of ambient PM_{2.5} across mountainous BC. Previous studies have found a particular deposition
287 process of PM_{2.5}, emitted from biomass burning, with long-distance transport (Ward et al.,
288 1991; Sapkota et al., 2005). We should emphasize that terrain can play an influential role in
289 the deposition, due to the aerodynamic characteristics of PM_{2.5} and the topographical effect
290 on wind flow. For example, the mountainous topography of BC, with its irregular terrain, can
291 result in uneven distribution of air pressure that further influences near-surface wind. The
292 effect of local terrain on PM_{2.5} dispersion due to its impact on wind dynamics has also been
293 found in another study in mountainous areas (Shi et al., 2017). A considerable fraction of PM_{2.5}
294 is therefore expected to be trapped by the leeward side of mountains, valleys, canyons and
295 basins (Steyn et al., 2013) under the typical transport process of air pollutants. Urban areas
296 with high aerodynamic surface roughness may also have influence similar to this topographical
297 effect on the deposition of PM_{2.5} from wildfires (Landsberg, 1981). These findings indicate that
298 regions across BC with lower altitude and with poorer air dispersion due to topographical
299 effects may be areas with higher PM_{2.5} concentration. In addition, these facts may also partly
300 explain the lower contribution of monthly coarse spatial resolution (2.5 degree latitude x 2.5
301 degree longitude) and monthly wind speed in modelling based on variable importance analysis,
302 while another reason may be the coarse spatial resolution (2.5 degree) of predictors derived
303 from NCEP/NCAR re-analysis data. Due to this resolution, it cannot represent micro-scale

304 topographical effects on air pollution transport and deposition. Some mountain valleys in BC
305 have high temperatures and little rainfall during the summer, and become dry enough to have
306 near-desert conditions with substantial amounts of dust suspended in the atmosphere, which
307 is also contributed to the high PM_{2.5} concentrations of valleys. An isolated cluster of high
308 PM_{2.5} in the Greater Vancouver Area and its surrounding regions was also observed, which has
309 not been shown in other BC cities. This can be attributed to the large population and
310 corresponding industrial, traffic and domestic emissions over this region.

311 Furthermore, CV-RMSE of this study was lower than previous research in other areas (Liu
312 et al., 2009; Song et al., 2014; Kloog et al., 2014; You et al., 2015; Reid et al., 2015; Liu et al.,
313 2005), partially indicating better air quality of BC compared to other regions. In contrast, a
314 lower CV-R² was found, which may be the result of extreme wildfire events in BC leading to
315 data with high PM_{2.5} concentration values as outliers in modelling.

316 **5.2 Advantages and Limitations**

317 In this study, optimization of machine learning models can effectively reduce the
318 sensitivity of the model tree to data noise with uncertainty; while the evaluation of eight
319 machine learning algorithms for modelling indicated that ensemble machine learning can
320 improve the accuracy of ground-level PM_{2.5} prediction. In addition, weather stations were
321 generally designed under government protocols, resulting in a sparse and uneven distribution.
322 This, as well as the strong variation in topography across the study area, makes it unsuitable
323 to apply conventional geostatistical methods such as spatial interpolation for mapping the
324 spatial variability of environmental variables (e.g. temperature and humidity), while these
325 maps should be the input layers for air quality prediction. In this study, we provided an

326 alternative, in which the use of LST and atmospheric water vapor derived from satellite images
327 can be substitutes for temperature and humidity maps.

328 There were areas with data missing from the prediction (Fig. 6). These were mainly the
329 high-altitude areas covered with perennial snow, because the Dark Target algorithm for AOD
330 retrieval was designed for areas with lower surface reflectance under a clear sky. For areas
331 with high surface reflectance values (e.g. snow coverage and desert), null values of AOD data
332 would be found. In addition, AOD values surrounding the missing data were generally high,
333 because AOD in such areas could be easily overestimated by the Dark Target algorithm,
334 especially in areas with high surface brightness and low vegetation coverage (Levy et al., 2010).
335 These became the areas with missing values of $PM_{2.5}$ concentration across snow coverage in
336 this study, and there were extremely high values of $PM_{2.5}$ concentration surrounding these
337 areas with missing data, especially those areas just below the snowline with lower vegetation
338 coverage. The issue of missing data is especially noticeable in winter, as mountainous BC was
339 covered by snow, resulting in high surface reflectance, and this area was also constantly
340 covered by clouds due to the relatively humid weather in wintertime, resulting in
341 spatiotemporal incompleteness of $PM_{2.5}$ estimation.

342 In addition, the $PM_{2.5}$ concentration over BC showed high values both in western high
343 mountains and the Fraser River Delta. The principal sources of $PM_{2.5}$ is likely different between
344 these areas. In mountain areas high $PM_{2.5}$ concentration is mostly caused by wildfires, while
345 in the Fraser River Delta high $PM_{2.5}$ concentration is caused by human activity. Due to the lack
346 of the chemical characteristics of particulate matter, we cannot perform a chemical analysis of
347 fine particulate matter over these regions. Further study with field measurement should be

348 applied to observe personal and ambient exposure of PM_{2.5} from multiple sources. However,
349 this future study will be limited by the accessibility of field measurement and the potential
350 bias from indoor-outdoor exchange of air pollution.

351 **6 Conclusions**

352 In this study, we evaluated the abilities of machine learning techniques to estimate the
353 monthly concentrations of ground-level PM_{2.5} between 2001 and 2014, based on eight
354 algorithms with predictors derived from remote sensing and meteorological re-analysis data.
355 Predictions from these algorithms were evaluated by a 10-fold cross-validation, with CV-RMSE
356 ranging from 2.64µg/m³ to 3.25µg/m³ and CV-R² ranging from 0.23-0.49. Among all, Cubist
357 had the best performance (CV-RMSE=2.64µg/m³, CV-R²=0.48). A series of maps were
358 produced for representing the monthly PM_{2.5} concentrations across BC, which can be
359 reference information on intra-province air pollution over 14 years for further air quality
360 monitoring and public health surveillance. In conclusion, selection of appropriate machine
361 learning algorithms for modelling can improve the accuracy in PM_{2.5} estimation, while using
362 satellite-derived data as predictors can minimize the spatial bias compared with use of
363 traditional datasets retrieved from weather stations.

364 Recently, deep learning technology has attracted much attention in various fields.
365 Compared with conventional machine learning technology, deep learning can provide better
366 accuracy but requires a large amount of training data (Camilleri and Prescott, 2017; Ravi et al.,
367 2017). Due to the limited number of air quality stations, there are not enough samples to
368 sufficiently train deep learning models. Therefore it is a big challenge to adopt deep learning
369 technology to map PM_{2.5} at the present stage. In the future, if the big training data requirement

370 of deep learning can be resolved, it is expected to achieve improved estimation of PM_{2.5}
371 concentration from remote sensing data. The method used in this study with the combination
372 of machine learning and multi-source variables was a preliminary attempt to map PM_{2.5}
373 concentration with the currently available data and suitable machine learning methods. The
374 method proposed in this paper could also be applied to other complex terrain regions with
375 sparse distributed air quality stations. Due to the limitation of AOD retrieval algorithms, the
376 remotely sensed AOD data have coarse spatial resolutions. Re-analysis data have even coarser
377 resolutions. The low spatial resolution of datasets restricts the application of this method on a
378 small scale (e.g. city scale).

379

380 **Acknowledgments**

381 This work was supported by the Social Sciences Foundation of the Ministry of Education
382 of China (Grant No. 17YJCZH205) and the National Key Research and Development Program of
383 China (2017YFB0503903-4). We would like to thank the Land Processes Distributed Active
384 Archive Center (LPDAAC) and Level-1 and Atmosphere Archive & Distribution System (LAADS)
385 for providing MODIS data, US Geological Survey (USGS) for providing SRTM/DEM data, and
386 National Oceanic and Atmospheric Administration (NOAA)/ Earth System Research Laboratory
387 (ESRL) for providing NCEP Reanalysis data. Man Sing Wong thanks the support in part by a
388 grant from the General Research Fund (project ID: 15205515); and a grant of PolyU 1-ZVFD
389 from the Research Institute for Sustainable Urban Development, the Hong Kong Polytechnic
390 University. We also thank the two reviewers for their valuable comments and suggestions.

391

392 **References**

- 393 Atkinson, R. W., Kang, S., Anderson, H.R., Mills, I.C., Walton, H.A., 2014. Epidemiological time
394 series studies of PM2.5 and daily mortality and hospital admissions: a systematic review
395 and meta-analysis. *Thorax* 69, 660–665
- 396 B.C. Wildfire Management Branch. 2014. Proactive Wildfire Threat Reduction. Accessed June
397 15, 2017. [http://docs.openinfo.gov.bc.ca/d63519414a_response_package_fnr-2014-](http://docs.openinfo.gov.bc.ca/d63519414a_response_package_fnr-2014-00274.pdf)
398 [00274.pdf](http://docs.openinfo.gov.bc.ca/d63519414a_response_package_fnr-2014-00274.pdf)
- 399 Bennett, K.P., Campbell, C., 2000. Support vector machines: hype or hallelujah? *SIGKDD Explor.*
400 2, 1–13.
- 401 Breiman, L., 2001. Random forests. *Mach. Learn.* 45, 5–32.
- 402 Burden, F., Winkler, D., 2008. Bayesian regularization of neural networks. *Methods Mol. Biol.*
403 458, 25–44.
- 404 Camilleri, D. Prescott, T., 2017. Analysing the limitations of deep learning for developmental
405 robotics. In: *Biomimetic and Biohybrid Systems. 6th International Conference, Living*
406 *Machines 2017, Stanford, CA, USA.*
- 407 Chen, B., Song, Y., Jiang, T., Chen, Z., Huang, B., Xu, B., 2018. Real-time estimation of population
408 exposure to PM2.5 using mobile-and station-based big data. *Int. J. Environ. Res. Public*
409 *Health* 15, 573.
- 410 Chen, T., Guestrin, C., 2016. XGBoost: A scalable tree boosting system. *Proceedings of the 22nd*
411 *ACM SIGKDD International Conference on Knowledge Discovery and Data Mining*, 785-
412 789.
- 413 Chu, H.J., Huang, B., Lin, C.Y., 2015. Modeling the spatio-temporal heterogeneity in the PM10-

414 PM2.5 relationship. *Atmos. Environ.* 102, 176–182.

415 Chu, Y., Liu, Y., Li, X., Liu, Z., Lu, H., Lu, Y., Mao, Z., Chen, X., Li, N., Ren, M., Liu, F., Tian, L., Zhu,
416 Z., Xiang, H., 2016. A review on predicting ground PM2.5 concentration using satellite
417 aerosol optical depth. *Atmosphere* 7, 129.

418 Crouse, D.L., Philip, S., van Donkelaar, A., Martin, R.V., Jessiman, B., Peters, P.A., Weichenthal,
419 S., Brook, J.R., Hubbell, B., Burnett, R.T., 2016. A new method to jointly estimate the
420 mortality risk of long-term exposure to fine particulate matter and its components. *Sci.*
421 *Rep.* 6, 18916.

422 Deters, J.K., Zalakeviciute, R., Gonzalez, M., ybarczyk Y., 2017. Modeling PM2.5 urban pollution
423 using machine learning and selected meteorological parameters. *J. Elect. Comput. Eng.*
424 2017, 1-14

425 Di, Q., Koutrakis, P., Schwartz, J., 2016. A hybrid prediction model for PM2.5 mass and
426 components using a chemical transport model and land use regression. *Atmos. Environ.*
427 131, 390–399.

428 Engel-Cox, J.A., Holloman, C.H., Coutant, B.W., Hoff, R.M., 2004. Qualitative and quantitative
429 evaluation of MODIS satellite sensor data for regional and urban scale air quality. *Atmos.*
430 *Environ.* 38, 2495–2509.

431 Friedman, J.H., 1991. Multivariate Adaptive Regression Splines. *Ann. Stat.* 19, 1–67.

432 Friedman, J.H., 2001. Greedy function approximation: a gradient boosting machine. *Ann. Stat.*
433 29, 1189–1232.

434 He, Q., Huang, B., 2018. Satellite-based high-resolution PM2.5 estimation over the Beijing-
435 Tianjin-Hebei region of China using an improved geographically and temporally weighted

436 regression model. *Environ. Pollut.* 236, 1027–1037.

437 Helsel, D. R., Hirsch, R. M., 1992. *Statistical Methods in Water Resources*, 296–299. Amsterdam:
438 Elsevier.

439 Henderson, S.B., Brauer, M., MacNab, Y.C., Kennedy, S.M., 2011. Three measures of forest fire
440 smoke exposure and their associations with respiratory and cardiovascular health
441 outcomes in a population-based cohort. *Environ. Health Perspect.* 119, 1266–1271.

442 Houborg, R., McCabe, M.F., 2018. A hybrid training approach for leaf area index estimation via
443 Cubist and random forests machine-learning. *ISPRS J. Photogramm. Remote Sens.* 135,
444 173–188.

445 Hsu, C.W., Chang, C.C., Lin, C.J., 2003. *A practical guide to support vector classification*.

446 Hu, X., Waller, L.A., Al-Hamdan, M.Z., Crosson, W.L., Estes, M.G., Jr, Estes, S.M., Quattrochi,
447 D.A., Sarnat, J.A., Liu, Y., 2013. Estimating ground-level PM_{2.5} concentrations in the
448 southeastern U.S. using geographically weighted regression. *Environ. Res.* 121, 1–10.

449 Hu, X., Belle, J.H., Xia, M., Wildani, A., Waller, L., Strickland, M., Liu Y., 2017. Estimating pm_{2.5}
450 concentrations in the conterminous United States using the random forest approach.
451 *Environ. Sci. Technol.* 51, 6936–6944.

452 Jiang M., Sun W., Yang G., Zhang D., 2017. Modelling seasonal GWR of daily PM_{2.5} with proper
453 auxiliary variables for the Yangtze River Delta. *Remote Sens.* 9, 346.

454 John, R., Chen, J., Giannico, V., Park, H., Xiao, J., Shirkey, G., Ouyang, Z., Shao G., Laforteza, R.,
455 Qi, J., 2018. Grassland canopy cover and aboveground biomass in Mongolia and Inner
456 Mongolia: Spatiotemporal estimates and controlling factors. *Remote Sens. Environ.* 213,
457 34–48.

458 Kan, H., Chen, R., Tong, S., 2012. Ambient air pollution, climate change, and population health
459 in China. *Environ. Int.* 42, 10–19.

460 Kloog, I., Sorek-Hamer, M., Lyapustin, A., Coull, B., Wang, Y., Just, A. C., Schwartz, J., Broday, D.
461 M., 2015. Estimating daily pm 2.5, and pm 10, across the complex geo-climate region of
462 Israel using MAIAC satellite-based AOD data. *Atmos. Environ.* 122, 409–416.

463 Kloog, I., Koutrakis, P., Coull, B.A., Lee, H.J., Schwartz, J., 2011. Assessing temporally and
464 spatially resolved PM2.5 exposures for epidemiological studies using satellite aerosol
465 optical depth measurements. *Atmos. Environ.* 45, 6267–6275.

466 Krstic, N., Henderson, S.B., 2015. Use of MODIS data to assess atmospheric aerosol before,
467 during, and after community evacuations related to wildfire smoke. *Remote Sens. Environ.*
468 166, 1–7.

469 Lai, H.K., Tsang, H., Thach, T.Q., Wong, C.M., 2014. Health impact assessment of exposure to
470 fine particulate matter based on satellite and meteorological information. *Environ. Sci.*
471 *Process. Impact* 2014, 16, 239–246.

472 Landsberg, H.E., 1981. *The urban climate* (Vol. 28). Academic Press.

473 Lary, D.J., Lay, T., Sattler, B., 2015. Using machine learning to estimate global PM2.5 for
474 environmental health studies, *Environ. Health Insights* 9, 41–52.

475 Lee, H.J., Chatfield, R.B., Strawa, A.W., 2016. Enhancing the applicability of satellite remote
476 sensing for PM2.5 estimation using MODIS deep blue AOD and land use regression in
477 California, United States. *Environ. Sci. Technol.* 50, 6546–6555.

478 Lee, H.J., Liu, Y., Coull, B. A., Schwartz, J., Koutrakis, P., 2011. A novel calibration approach of
479 MODIS AOD data to predict PM2.5 concentrations. *Atmospheric Chem. Phys.* 11, 7991–

480 8002.

481 Levy, R.C., Remer, L.A., Kleidman, R.G., Mattoo, S., 2010. Global evaluation of the collection 5
482 modis dark-target aerosol products over land. *Atmospheric Chem. Phys.*, 10, 10399–
483 10420.

484 Liu, J., Li, W., Wu, J., Liu, Y. 2018. Visualizing the intercity correlation of PM2.5 time series in
485 the Beijing-Tianjin-Hebei region using ground-based air quality monitoring data. *PloS one*,
486 13, e0192614.

487 Liu, Y., 2014. Mapping annual mean ground-level PM2.5 concentrations using multiangle
488 imaging spectroradiometer aerosol optical thickness over the contiguous United States.
489 *J. Geophys. Res.* 109, D22.

490 Liu Y., Paciorek C.J., Koutrakis P., 2009. Estimating regional spatial and temporal variability of
491 PM2.5 concentrations using satellite data, meteorology, and land use information.
492 *Environ. Health Perspect.* 117, 886–892.

493 Liu, Y., Franklin, M., Kahn, R., Koutrakis, P., 2007. Using aerosol optical thickness to predict
494 ground-level PM 2.5 concentrations in the St. Louis area: a comparison between MISR
495 and MODIS. *Remote Sens. Environ.* 107, 33–44.

496 Ma, Z., Hu, X., Huang, L. Bi, J., Liu, Y., 2014. Estimating ground-level PM2.5 in China using
497 satellite remote sensing. *Environ. Sci. Technol.* 48, 7436–7444.

498 McLean, K.E., Yao, J., Henderson, S.B., 2015. An evaluation of the British Columbia Asthma
499 Monitoring System (BCAMS) and PM2.5 exposure metrics during the 2014 forest fire
500 season. *Int. J. Environ. Res. Public Health* 12, 6710–6724.

501 Mukai, S., Sano, I., Satoh, M., Holben, B.N., 2006. Aerosol properties and air pollutants over

502 an urban area. *Atmos. Res.* 82, 643–651.

503 Natunen, A., Arola, A., Mielonen, T., Huttunen, J., Komppula, M., Lehtinen, K.E.J., 2010. A
504 multi-year comparison of PM_{2.5} and AOD for the Helsinki region. *Boreal Environ. Res.* 15,
505 544–552

506 Ngufor, C., Murphree, D., Upadhyaya, S., Madde, N., Kor, D., Pathak, J., 2015. Effects of plasma
507 transfusion on perioperative bleeding complications: a machine learning approach. *Stud.*
508 *Health Technol. Inform.* 216, 721–725.

509 Ostro, B., Malig, B., Broadwin, R., Basu, R., Gold, E.B., Bromberger, J.T., Derby, C., Feinstein, S.,
510 Greendale, G. Jackson, E., Kravitz, H.M., Matthews, K.A., Sternfeld, B., Tomey, K., Green,
511 R.R., Green. R., 2014. Chronic PM_{2.5} exposure and inflammation: determining sensitive
512 subgroups in mid-life women. *Environ. Res.* 132, 168–175.

513 Paciorek, C.J., Liu, Y., Moreno-Macias, H., Kondragunta, S., 2008. Spatiotemporal associations
514 between GOES aerosol optical depth retrievals and ground-level PM_{2.5}. *Environ. Sci.*
515 *Technol.* 42, 5800–5806.

516 R Core Development Team, 2016. R: A language and environment for statistical computing. R
517 Foundation for Statistical Computing, Vienna, Austria.

518 Ravi, D., Wong, C., Deligianni, F., Berthelot, M., Andreu-Perez, J., Lo, B., Yang, G.Z. 2017. Deep
519 learning for health informatics. *IEEE J. Biomed. Health Inform.* 21, 4–21.

520 Reid C.E., Jerrett, M., Petersen, M.L., Pfister, G.G., Morefield, P.E., Tager, I.B., Raffuse, S.M.,
521 Balmes, J.R., 2015. Spatiotemporal prediction of fine particulate matter during the 2008
522 Northern California wildfires using machine learning. *Environ. Sci. Technol.* 49,
523 3887–3896

524 RuleQuest., 2018. Data mining with Cubist, <https://www.rulequest.com/cubist-info.html>

525 Sapkota, A., Symons, J.M., Kleissl, J., Wang, L., Parlange, M.B., Ondov, J., Breyse, P.N., Buckley,
526 T.J., 2005. Impact of the 2002 Canadian forest fires on particulate matter air quality in
527 Baltimore City. *Environ. Sci. Technol.* 39, 24–32.

528 Saunders, R.O., Kahl, J.D.W., Ghorai, J.K., 2014. Improved estimation of PM_{2.5} using Lagrangian
529 satellite-measured aerosol optical depth. *Atmos. Environ.* 91, 146–153.

530 Schaap, M., Apitley, A., Timmermans, R.M.A., Koelemeijer, R.B.A., de Leeuw G., 2009.
531 Exploring the relation between aerosol optical depth and PM_{2.5} at Cabauw, the
532 Netherlands. *Atmos. Chem. Phys.* 9, 909–925.

533 Shi, Y., Ho, H.C., Xu, Y., Ng, E., 2018. Improving satellite aerosol optical Depth-PM_{2.5}
534 correlations using land use regression with microscale geographic predictors in a high-
535 density urban context. *Atmos. Environ.* Doi: 10.1016/j.atmosenv.2018.07.021.

536 Shi, Y., Lau, K.K.L., Ng, E., 2017. Incorporating wind availability into land use regression
537 modelling of air quality in mountainous high-density urban environment. *Environ. Res.*
538 157, 17–29.

539 Song, W., Jia, H., Huang, J., Zhang, Y., 2014, A satellite-based geographically weighted
540 regression model for regional PM_{2.5} estimation over the Pearl River Delta region in China.
541 *Remote Sens. Environ.* 154, 1–7.

542 Steyn, D.G., De Wekker, S.F., Kossmann, M., Martilli, A., 2013. Boundary layers and air quality
543 in mountainous terrain. In *Mountain Weather Research and Forecasting*. Springer
544 Netherlands, pp. 261–289.

545 Tibshirani, R., 1996. Regression shrinkage and selection via the lasso. *J. R. Stat. Soc. Series B*

546 Stat. Methodol. 58, 267–288.

547 van Donkelaar A., Martin R.V., Park R. J., 2006. Estimating ground-level pm2.5 using aerosol
548 optical depth determined from satellite remote sensing. *J. Geophys. Res.* 111, D21.

549 Wang, B., Chen, Z., 2016. High-resolution satellite-based analysis of ground-level PM2.5 for
550 the city of Montreal. *Sci. Total Environ.* 541, 1059–1069.

551 Wang, J., Christopher, S.A., 2003. Intercomparison between satellite derived aerosol optical
552 thickness and PM2.5 mass: implications for air quality studies, *Geophys. Res. Lett.* 30,
553 2095.

554 Wang, Y., Shi, L., Lee, M., Liu, P., Di, Q., Zanobetti, A., Schwartz, J.D., 2017. Long-term exposure
555 to PM2.5 and mortality among older adults in the Southeastern US. *Epidemiology* 28,
556 207–214.

557 Ward, D.E., Hardy, C.C., 1991. Smoke emissions from wildland fires. *Environ. Int.* 17, 117-134.

558 Xie, Y., Wang, Y., Zhang, K., Dong, W., Lv, B., Bai, Y., 2015. Daily estimation of ground-level
559 PM2.5 concentrations over Beijing using 3km resolution MODIS AOD. *Environ. Sci.*
560 *Technol*, 19, 12280–12288.

561 Wotton, B.M., Nock, C.A., Flannigan, M.D., 2010. Forest fire occurrence and climate change in
562 Canada. *Int. J. Wildland Fire* 19, 253–271.

563 Wu, J., Li, J., Peng, J., Li, W., Xu, G., Dong, C., 2015. Applying land use regression model to
564 estimate spatial variation of PM2.5 in Beijing, China. *Environ. Sci. Pollut. Res. Int.* 22,
565 7045-7061.

566 Wu, J., Yao, F., Li, W., Si, M., 2016. VIIRS-based remote sensing estimation of ground-level
567 PM2.5 concentrations in Beijing-Tianjin-Hebei: A spatiotemporal statistical model.

568 Remote Sens. Environ., 184, 316–328.

569 Xin, J., Zhang, Q., Wang, L., Gong, C., Wang, Y., Liu, Z., Gao, W., 2014. The empirical relationship
570 between the PM2.5 concentration and aerosol optical depth over the background of
571 North China from 2009 to 2011. Atmos. Res. 128, 179–188.

572 Yao, F., Si, M., Li, W., Wu, J., 2018a. A multidimensional comparison between MODIS and VIIRS
573 AOD in estimating ground-level PM2.5 concentrations over a heavily polluted region in
574 China. Sci. Total Environ 618, 819-828.

575 Yao, J., Raffuse, S.M., Brauer, M., Williamson, G.J., Bowman, D.M., Johnston, F.H., Henderson,
576 S.B., 2018b. Predicting the minimum height of forest fire smoke within the atmosphere
577 using machine learning and data from the CALIPSO satellite. Remote Sens. Environ. 206,
578 98–106.

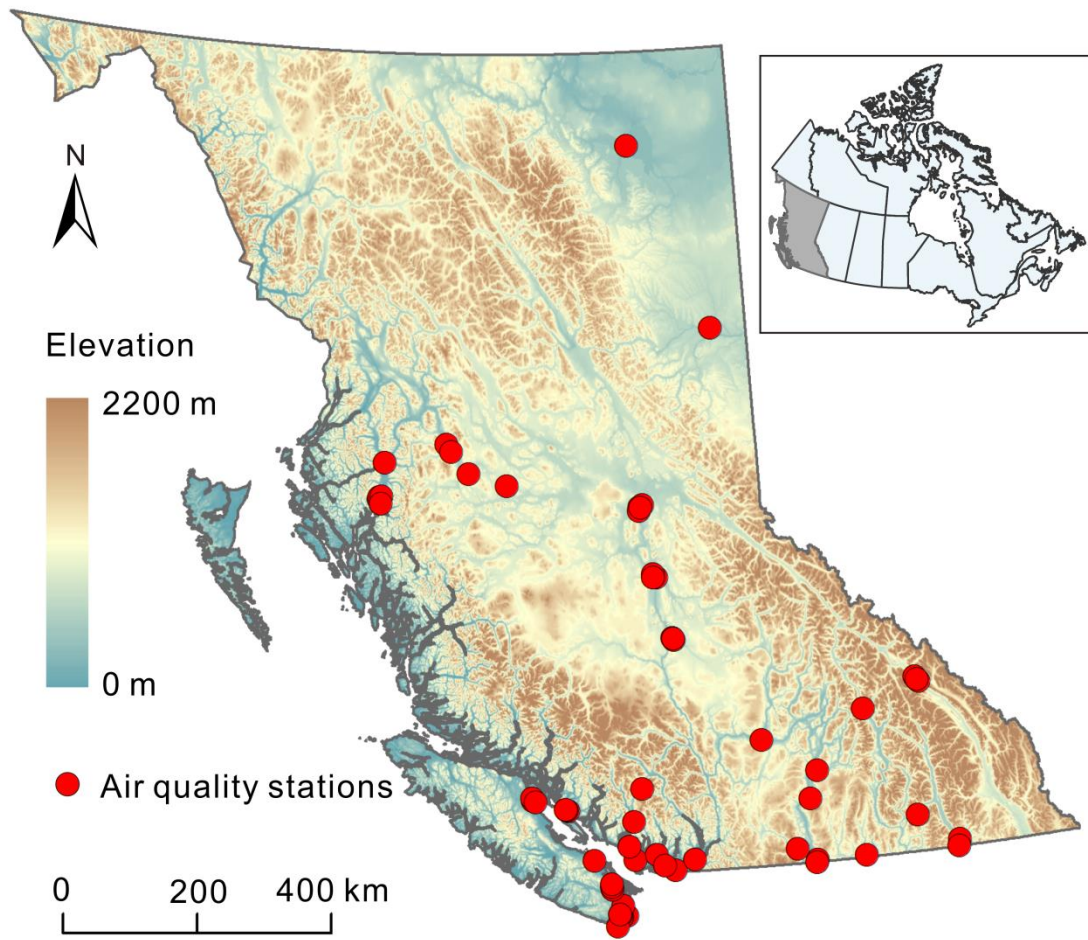
579 You, W., Zang, Z., Pan, X., Zhang, L., Chen, D., 2015. Estimating pm2.5 in Xi'an, China using
580 aerosol optical depth: a comparison between the MODIS and MISR retrieval models. Sci.
581 Total Environ. 505, 1156–1165.

582 You, W., Zang, Z., Zhang, L., Li, Y., Pan, X., Wang, W., 2016. National-scale estimates of ground-
583 level PM2.5 concentration in China using geographically weighted regression based on 3
584 km resolution MODIS AOD. Remote Sens. 8, 184.

585 Zheng, Y., Zhang, Q., Liu, Y., Geng, G., He, K., 2016. Estimating ground-level PM2.5
586 concentrations over three megalopolises in China using satellite-derived aerosol optical
587 depth measurements. Atmos. Environ. 124, 232–242.

588 Zhan, Y., Luo, Y., Deng, X., Chen, H., Grieneisen, M.L., Shen, X., Zhu, L., Zhang, M., 2017.
589 Spatiotemporal prediction of continuous daily PM2.5, concentrations across China using

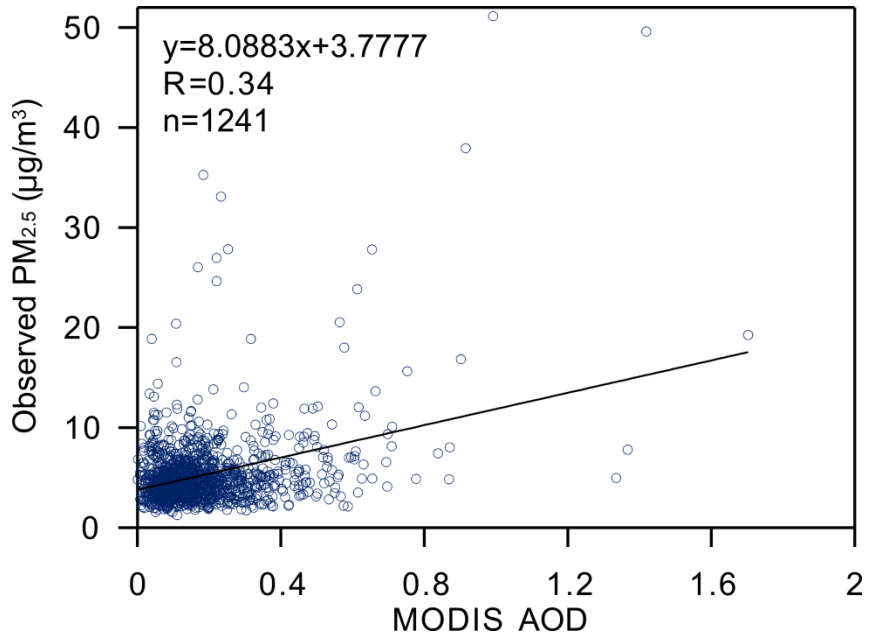
590 a spatially explicit machine learning algorithm. *Atmos. Environ.* 155, 129–139.



591

592

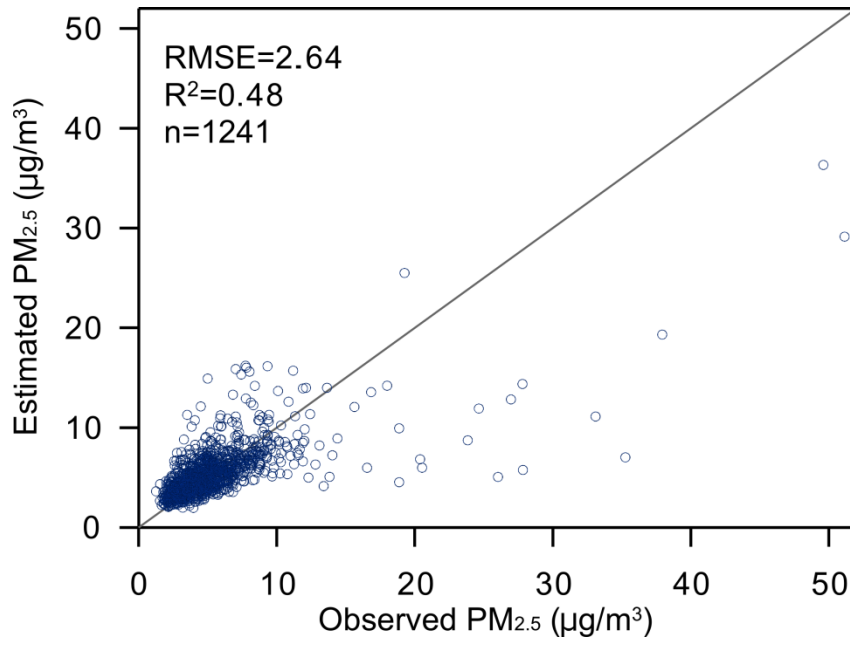
Fig. 1. Study Site. Red dots represent the location of air quality stations across BC.



593

594 Fig.2 Empirical relationship between PM_{2.5} and AOD. X-axis indicated the AOD values derived

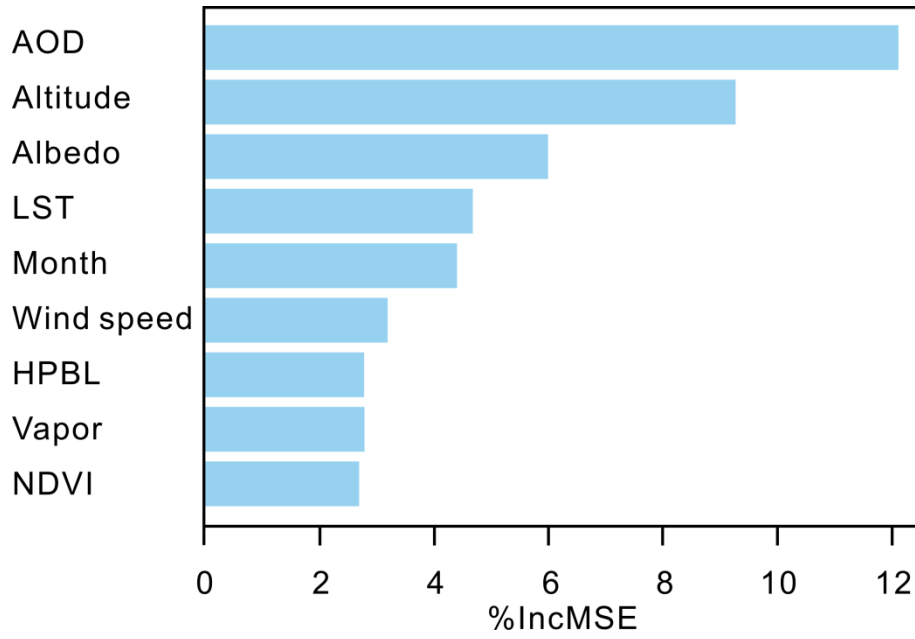
595 from MODIS dataset. Y-axis indicated the PM_{2.5} retrieved from the air quality stations.



596

597

Fig. 3 Comparison between observed and estimated PM_{2.5} using Cubist.



598

599

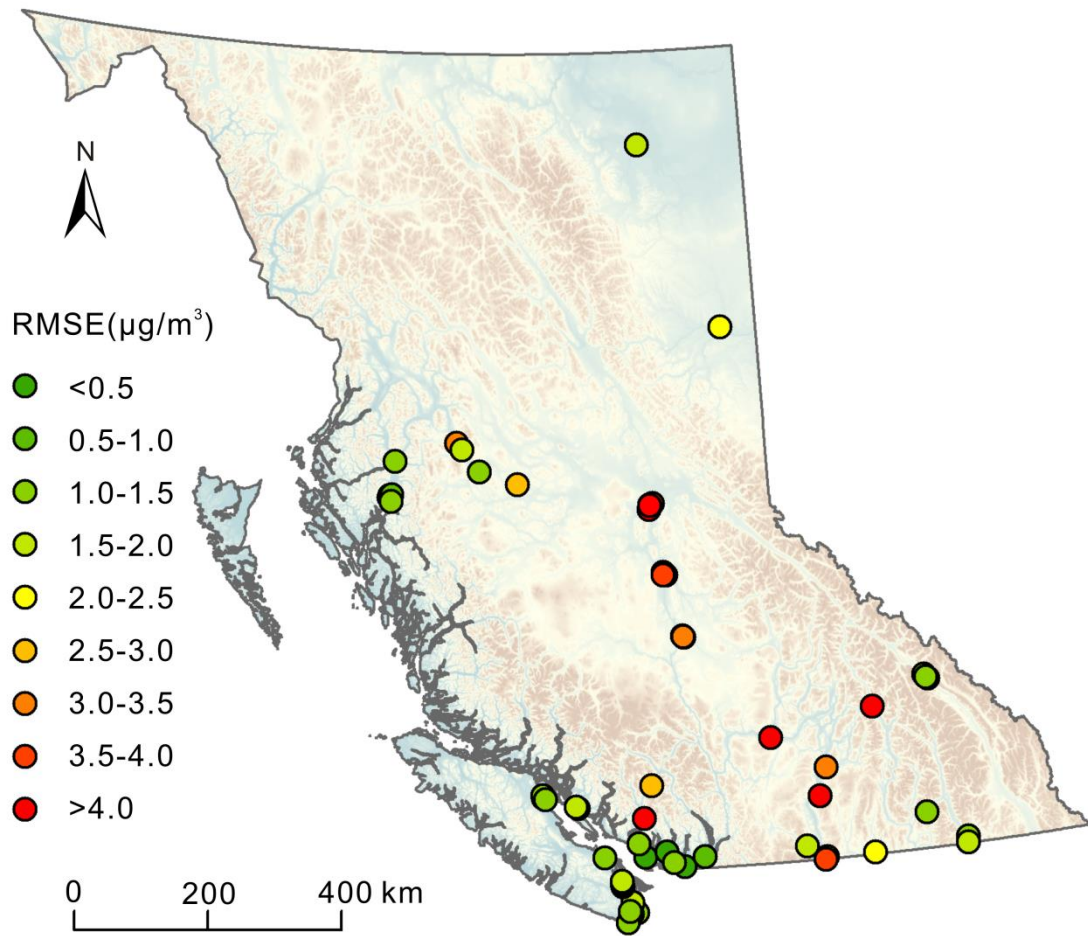
Fig. 4 Variable importance analysis (Cubist Model). Y-axis indicated the predictors for

600

predicting $PM_{2.5}$. X-axis indicated the percentage increase in mean square error (%IncMSE)

601

without using the corresponding predictor.

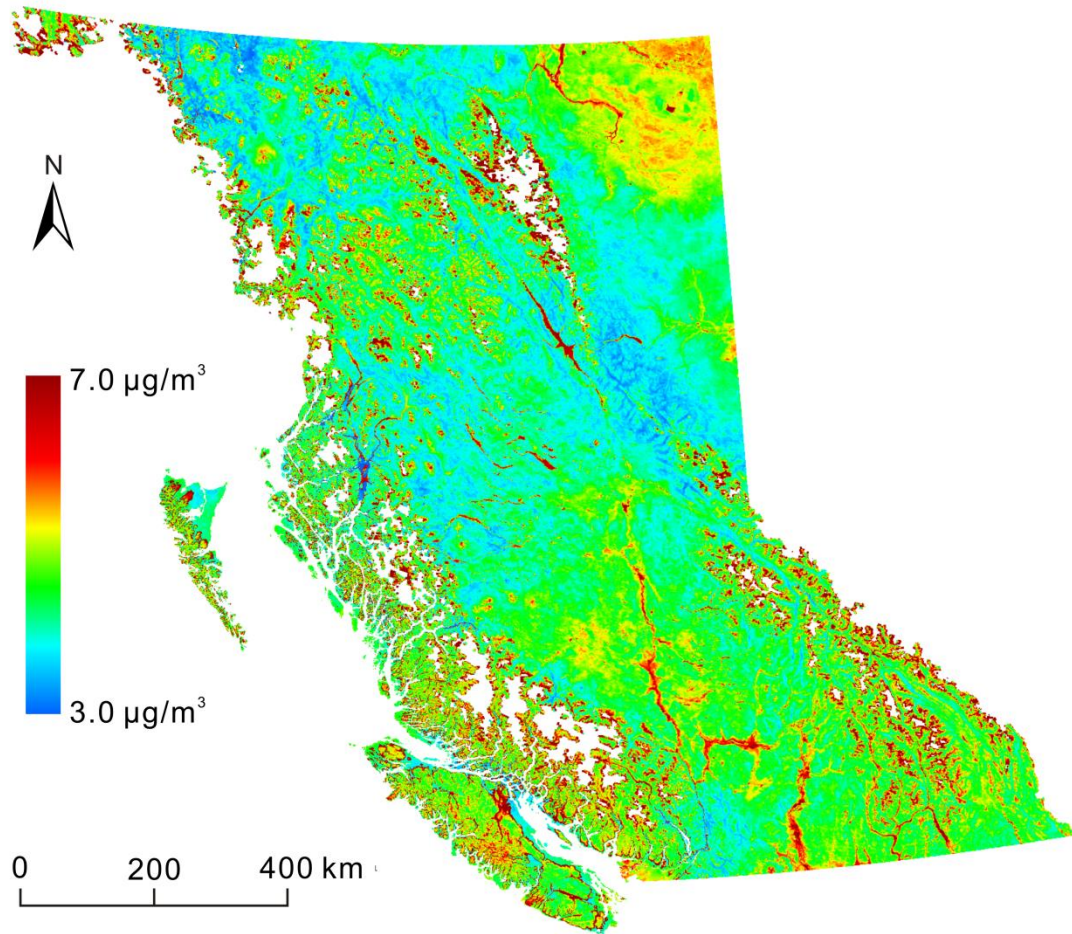


602

603 **Fig. 5** Location-based root mean square error (RMSE) of estimated $\text{PM}_{2.5}$. Red indicated an air

604 quality station with higher RMSE, and green indicated a station with lower RMSE after a

605 comparison with observed data.



606

607

Fig. 6 Average of ground-level PM_{2.5} concentration across BC (2001-2014)

608 **Table 1** Information on datasets used for PM2.5 estimation

Dataset	Spatial resolution	Temporal resolution	Scenes	Derived predictors
MOD04_3k	3km	Daily	25350	AOD
MOD05_L2	1km	Daily	22198	Vapor
MOD11A1	1km	Daily	25369	LST
MOD13A3	1km	Monthly	1677	NDVI
MCD43B3	1km	16 days	6394	albedo
NCAR/NCEP re-analysis	2.5°	Monthly	/	HPBL, wind speed
SRTM DEM	90m	/	/	elevation

609

610 **Table 2** Accuracy of PM_{2.5} prediction of each machine learning model.

Model	CV-RMSE ($\mu\text{g}/\text{m}^3$)	CV-R ²
MLR	3.24	0.22
BRNN	3.04	0.31
SVM	3.13	0.30
LASSO	3.20	0.24
MARS	3.05	0.31
RF	2.67	0.49
XGBoost	2.71	0.46
Cubist	2.64	0.48

611